Distributed Secondary Frequency Control in AC Microgrids with Lossy Electrical Networks

Siddhartha Nigam, Olaoluwapo Ajala, Madi Zholbaryssov, Alejandro D. Domínguez-García, Peter W. Sauer
ECE, University of Illinois at Urbana-Champaign
Email: {nigam4, ooajala2, zholbar1, aledan, psauer}@illinois.edu

***Abstract*—This paper presents a distributed control scheme for achieving secondary frequency control in AC microgrids. The control scheme is designed for microgrid electrical networks comprised of distribution lines with equal/unequal resistance to reactance ratio; in other words, it works well even when ohmic losses are taken into account in the microgrid electrical network. The control problem is formulated and an overview of the proposed distributed secondary frequency control scheme is provided. A criterion for choosing controller gains that stabilize the system frequency is also provided. Finally, results on the testing of the control scheme on a controller hardware-in-the loop (C-HIL) testbed are provided.**

***Index Terms*—Lossy Microgrid; Distributed secondary frequency control; Controller hardware-in-the-loop**

I. Introduction

Over the last few years, the microgrid concept has been shown to be a promising approach to enable the efficient integration and management of distributed energy resources (DERs) [1], [2], [3]. Loosely speaking, a microgrid can be defined as a network of interconnected loads and DERs, within clearly defined geographic boundaries, that can be viewed as a single controllable entity with respect to the grid, and can operate in grid-connected or grid-islanded modes [4]. In grid-islanded mode, frequency control is a major problem because prevalence of inverter-interfaced DERs leaves the microgrid with low or no rotating inertia [5]. Among the various frequency controls, a key one is secondary frequency control [6], which ensures the system-wide frequency returns to its nominal value following any change in operating point of the microgrid.

Several secondary frequency control schemes for microgrids based on a centralized or decentralized decision-making approach have been proposed in the literature [7], [8]. Nevertheless, control schemes that are based on a distributed decision-making approach have gained some popularity among researchers in the last decade [9], [10], [11], [12]. It has been postulated that such schemes overcome limitations of centralized and decentralized alternatives in terms of their adaptability to additions/removals of DERs, and resilience against controller failures [12].

In [13], [14], distributed secondary frequency control schemes for islanded microgrids are presented, and the developments made by the authors are based on the assumption that all electrical lines in the network have an equal resistance to reactance ratio; this essentially reduces the problem to that of controlling an electrically lossless microgrid. In this work, however, we wish to take a step beyond this by presenting a distributed secondary frequency control scheme that does not require such assumption. We describe the relevant modifications to the control problem, as well as the modifications to the controller described in [14], in order to account for ohmic losses in the electrical network with the distribution lines having unequal resistance to reactance ratios. While in this paper we focus on AC microgrids with inverter-interfaced DERs, the proposed control scheme also works with any other generation mix. Furthermore, the proposed scheme requires the monitoring of only buses to which DERs are connected, as opposed to the scheme in [14] which requires the monitoring of all buses to which DERs and loads are connected.

To test the proposed distributed secondary frequency control scheme, a controller hardware-in-the loop (C-HIL) testbed is utilized. The C-HIL testbed comprises an emulated islanded AC microgrid, whose components, i.e., the electrical network and the DERs and loads connected to it are simulated using a Typhoon HIL real-time emulator (see [15], for details on a microgrid implementation using Typhoon HIL simulator). The model of the islanded microgrid is developed using high-order models of inverter-interfaced DERs [16]. Monitoring and control of the DERs is achieved through the use of several interconnected Arduino microcontrollers, which implement our distributed algorithms for microgrid secondary frequency control (see [10], [12], [14], for details on these algorithms). To achieve secondary frequency control, each Arduino microcontroller utilizes the information acquired, e.g., from measurements and other information obtained through exchanges with other nearby arduino devices, to perform successive computations and adjust the set-points of the DERs it controls accordingly.

The remainder of this paper is organized as follows. In Section II, we describe the secondary frequency control problem and the proposed distributed control scheme for AC microgrids with inverter-interfaced DERs. In Section III, we provide a description of the C-HIL setup for testing the proposed control scheme. In Section IV, we present the C-HIL testing results. Finally, in Section V, we provide concluding remarks.

II. Distributed Secondary Frequency Control

In this section, we first present the reduced-order model that was adopted in this work in order to formulate the

control problem. Afterwards, we describe the secondary frequency control problem for islanded microgrids equipped with inverter-interfaced resources. Finally, we present a distributed control scheme that can be utilized for solving the aforementioned secondary frequency control problem.

A. Microgrid Model

The reduced-order model utilized for developing the distributed secondary frequency control scheme is based on the following assumptions:

A1. the microgrid is a balanced three-phase system whose network is comprised of short transmission lines,
A2. all loads are constant power type,
A3. the DERs are interfaced via droop-controlled voltage source inverters,
A4. the frequency of each inverter is controlled using the frequency droop control laws described in [11], [17], [18],
A5. all the quantities are in per-unit, and the voltage magnitudes are maintained at 1 per-unit,
A6. the dynamics of the network, the inverter's filter, and the outer voltage controller comprise the fastest dynamic phenomena in the system,
A7. the dynamics of the outer voltage controller and inner current controller are much faster than those of the droop control, and
A8. the inverter reactive power capability is sufficient to support voltage control.

Let $\theta_i(t)$ represent the voltage phase angle at bus i, relative to a reference frame that rotates at some nominal frequency, e.g., 60 Hz. The net active power injection at bus i, $p_i(t)$, is given by:

$$p_i(t) := G_{ii} + \sum_{j\in\mathcal{N}_p(i)} \Big(G_{ij}\cos\big(\theta_i(t)-\theta_j(t)\big) + B_{ij}\sin\big(\theta_i(t)-\theta_j(t)\big)\Big), \tag{1}$$

where $\mathcal{N}_p(i)$ is the set of buses to which bus i is electrically connected, $-G_{ij}$ and $-B_{ij}$ represent the conductance and susceptance of the lines connecting buses i and j, respectively, and $G_{ii} := -\sum_{j\in\mathcal{N}_p(i)} G_{ij}$.

For the inverter-interfaced DER connected to bus $i \in \mathcal{V}_p^{(g)} := \{1,2,...,m\}$, let $u_i(t)$ represent the active power set-point, and let $\underline{u}_i$ and $\overline{u}_i$ represent its lower and upper limits for the active power set-point, respectively. Then, for each bus $i \in \mathcal{V}_p^{(g)} := \{1,2,...,m\}$ that a DER is connected to, we have that

$$D_i\dot{\theta}_i = u_i(t) - p_i(t), \qquad \underline{u}_i \le u_i(t) \le \overline{u}_i, \tag{2}$$

where D_i represents the frequency droop coefficient.

For the constant power load connected to bus $i \in \mathcal{V}_p^{(d)} := \{m+1, m+2, ..., n\}$, let $d_i(t)$ represent the total active power demand at bus i. Then, for each bus $i \in \mathcal{V}_p^{(d)} := \{m+1, m+2, ..., n\}$ that a load is connected to, we have that

$$0 = -d_i(t) - p_i(t). \tag{3}$$

B. The Secondary Frequency Control Problem

For the microgrid whose dynamics are described by the reduced-order model in (1) – (3), the secondary frequency control problem entails regulating the value of each $u_i(t)$, $i \in \mathcal{V}_p^{(g)}$ so that:

$$\dot{\theta}_i \to 0 \quad \text{as} \quad t \to \infty.$$

Let the average frequency error (AFE) be defined as follows:

$$\Delta\overline{\omega}(t) := \frac{\sum_{i=1}^n D_i\dot{\theta}_i}{\sum_{i=1}^n D_i}. \tag{4}$$

Let $l(t)$ represent the total losses in the system, which are given by

$$l(t) := \sum_{i=1}^n \sum_{j=1}^n G_{ij}\cos(\theta_i(t) - \theta_j(t). \tag{5}$$

Substituting (2) and (3) into (4) yields

$$\Delta\overline{\omega}(t) = \frac{\sum_{i\in\mathcal{V}_p^{(g)}} u_i(t) - \sum_{i\in\mathcal{V}_p^{(d)}} d_i(t) - l(t)}{\sum_{i=1}^n D_i}. \tag{6}$$

From (1), (3), and (5) it follows that:

$$\sum_{i\in\mathcal{V}_p^{(g)}} p_i(t) = \sum_{i\in\mathcal{V}_p^{(d)}} d_i(t) + l(t), \tag{7}$$

and therefore (6) can be simplified to:

$$\Delta\overline{\omega}(t) = \frac{\sum_{i\in\mathcal{V}_p^{(g)}} u_i(t) - \sum_{i\in\mathcal{V}_p^{(g)}} p_i(t)}{\sum_{i=1}^n D_i}. \tag{8}$$

We now make use of the AFE expression defined in (8) to describe the distributed secondary frequency control scheme that was developed and tested in this work.

C. Secondary Frequency Control Scheme

In our implementation of the distributed secondary frequency control scheme, time is discretized into rounds $r = 0, 1, 2...$, with each round having a fixed duration T_0. Thus, let

$$u_i[r] := u_i(t), \qquad t_r \le t < t_{r+1},$$

where t_r denotes the beginning of round r, and $t_{r+1} - t_r = T_0$; then, (8) can be rewritten as:

$$\Delta\overline{\omega}[r] = \overline{D}\left(\sum_{i\in\mathcal{V}_p^{(g)}} u_i[r] - \sum_{i\in\mathcal{V}_p^{(g)}} p_i[r] \right), \tag{9}$$

where $\overline{D} := \frac{1}{\sum_{i=1}^n D_i}$. Following from the distributed control scheme presented in [14], the active power set-point of generator $i \in \mathcal{V}_p^{(g)}$ can be adjusted according to:

$$e_i[r+1] = e_i[r] + \kappa_i\Delta\overline{\omega}[r], \tag{10}$$

$$u_i[r] = u_i^* + \alpha_i e_i[r], \tag{11}$$

where $e_i[0] = 0$, and α_i and κ_i are appropriately chosen gains. For the choice of gains α_i and κ_i in the lossy case, we make the following reasonable assumption.

Assumption: If the total resistive losses in the microgrid

change after a change in the DER active power set-points, the magnitude of the total change in resistive losses is less than that of the total change in generation set-points. In other words, for

$$\Delta u[r] := \sum_{i \in \mathcal{V}_p^{(g)}} (u_i[r] - u_i[r-1]),$$
$$\Delta l[r] := l[r] - l[r-1],$$

we have that:

$$|\Delta l[r]| \leq \gamma |\Delta u[r]|, \tag{12}$$

where $\gamma < 1$. Now, we state the following proposition (without a proof due to space limitations) to provide a criterion for choosing the controller gains.

Proposition: The controller provided in (10) and (11) converges geometrically fast at a rate $\mathcal{O}(a^r)$ if the controller gains satisfy the following relation:

$$\gamma \sum \alpha_i \kappa_i + \left| \sum (D_i + \alpha_i \kappa_i) \right| < a \sum D_i, \tag{13}$$

where $a \in (0, 1)$.

D. Distributed Implementation

Each DER adjusts its active power set-point according to (10) and (11), but in order to do so, the DERs will compute the AFE, $\Delta\overline{\omega}[r]$, in a distributed fashion. To this end, the microgrid is endowed with multiple, geographically dispersed, computing devices referred to as distributed control nodes. Each distributed control node can acquire information locally from its associated DER, e.g., for each $i \in \mathcal{V}_p^{(g)}$, a control node has access to the corresponding DER set point, $u_i[r]$, and active power injection, $p_i[r]$. In addition, the control nodes can exchange information among themselves. The distributed control nodes with which a particular node can communicate are referred to as the neighbors of that particular control node.

The control nodes use the information they acquire locally, e.g., from measurements, and via exchanges with their neighbors, as inputs to the so-called ratio consensus algorithm (see, e.g., [9], [12], [14]). Through the ratio-consensus algorithm, each control node computes the AFE in a distributed manner. Once the AFE is computed, its value is fed to the controller in (10)–(11), which will adjust the DER active set-points iteratively, eventually driving the AFE to zero. Below, we provide a brief overview of the ratio-consensus algorithm and explain how it fits in the distributed computation of the AFE.

1) The ratio consensus algorithm: The neighbors of control node i, i.e., the control nodes that node i communicates with bidirectionally, are represented by the set $\mathcal{N}_c(i)$. Each control node i maintains two internal states, y_i and z_i, which, at iteration k, it updates as follows:

$$y_i[k+1] = \sum_{j \in \mathcal{N}_c(i) \cup \{i\}} \frac{1}{|\mathcal{N}_c(j)| + 1} y_j[k], \tag{14}$$

$$z_i[k+1] = \sum_{j \in \mathcal{N}_c(i) \cup \{i\}} \frac{1}{|\mathcal{N}_c(j)| + 1} z_j[k]. \tag{15}$$

Each node i uses then $y_i[k]$ and $z_i[k]$ to compute $\gamma_i[k] = \frac{y_i[k]}{z_i[k]}$. This is repeated until a finite number of iterations, K, is completed when $\gamma_i[K]$ is close to $\frac{\sum_i y_i[0]}{\sum_i z_i[0]}$ for all i—the value of K can be determined also in a distributed fashion with the algorithm described in [19].

In order to compute the AFE in a distributed fashion, define

$$x_i[r] = u_i[r] - p_i[r], \ i \in \mathcal{V}_p^{(g)}, \tag{16}$$

then $\Delta\overline{\omega}[r] = \frac{\sum_{i \in \mathcal{V}_p} x_i[r]}{\sum_{i \in \mathcal{V}_p} D_i}$. Accordingly, if we set $y_i[0] = x_i[r]$ and $z_i[0] = D_i$ at the beginning of each round r, we have that

$$\lim_{k \to \infty} \frac{y_i[k]}{z_i[k]} = \Delta\overline{\omega}[r], \quad i \in \mathcal{V}_p^{(g)}.$$

Thus, using the ratio-consensus algorithm at each round r, each distributed control node can learn the value of $\Delta\overline{\omega}[r]$ and then use it to adjust the active power set-points of the DERs according to (10) and (11). While the ratio consensus formulation described here is not robust against communication packet drops, the variant of the ratio-consensus algorithm that is implemented in the C-HIL testbed is robust against packet drops (see [20], for details).

III. C-HIL Testing Setup of Distributed Frequency Control Scheme

In this section, we briefly describe the C-HIL testbed setup for testing the proposed distributed frequency control scheme. The C-HIL testbed is comprised of two layers, the physical layer and the cyber layer. The physical layer comprises a real-time emulation of an islanded AC microgrid network and the loads and DERs connected to it. The cyber layer comprises several control nodes implementing the distributed algorithms used for implementation of the distributed frequency control scheme. More details on the C-HIL testbed and its capabilities are provided in [21].

A. Physical Layer

The physical layer comprises a Typhoon HIL real-time emulator that is used to simulate the microgrid electrical power network and the DERs and loads connected to it. The Typhoon HIL hardware provides simulation step sizes as low as 0.5 μs that allows us to test various control schemes in a high-fidelity emulation setting. Specific details on the role of the Typhoon hardware in our C-HIL testbed are provided in [21]. The inverter-interfaced DERs are modeled using a thirteenth-order "averaged" model (see [16] for details). This high-order model captures all fast dynamics except for inverter switching. The microgrid electrical network that was emulated on the Typhoon HIL real-time emulator, and used for C-HIL testing of the distributed control scheme, is shown in Fig. 1. It consists of six buses; three of these have DERs connected to them, and the remaining ones have constant loads connected to them.

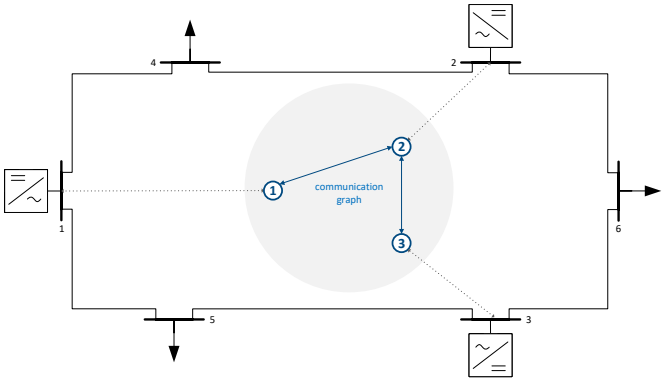

Fig. 1: 6-bus microgrid with 3-control nodes communicating with each other according to the communication graph highlighted in the figure.

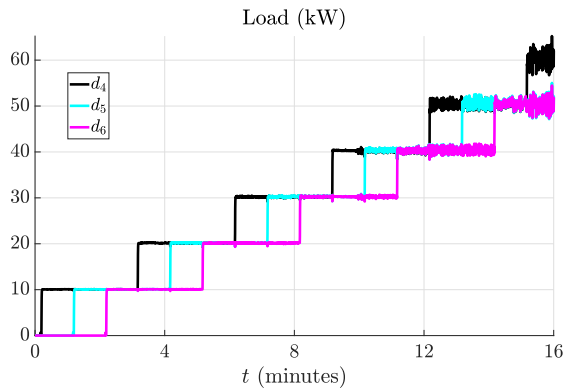

Fig. 2: Demand perturbation at bus 4, 5 and 6.

B. Cyber Layer

To monitor and control DERs in the emulated microgrid, three Arduino Due microcontrollers serve as the distributed control nodes. Each device is interfaced with an ethernet shield; this allows the control nodes to communicate with the Typhoon HIL device via the Modbus TCP/IP protocol so as to enable monitoring and control of DERs in the emulated microgrid. In addition, each control node also has a MaxStream XB24-DMCIT-250 revB XBee wireless module which allows the control nodes to communicate and exchange information with their neighbors.

The three DERs at bus 1, 2, and 3 are monitored and controlled by control nodes 1, 2 and 3, respectively, as shown in Fig. 1. Control node 2 monitors and controls the DER at bus 2 and can communicate bidirectionally with control nodes 1 and 3. Each control node implements the ratio consensus algorithm, and this enables to compute the AFE in a distributed fashion. The control nodes utilize the AFE together with (10)–(11) to update the DER set-points.

IV. Results

We start out by providing details on the microgrid network, DERs and loads. We then provide the initial DER and load set points. Afterwards, we provide the load demand perturbation profile used for testing the proposed control scheme. Finally, we present results depicting the system frequency response and the DER injections for two cases; first, without secondary frequency control scheme deployed and then, with it.

A. Active power profiles for DERs and loads

The rated capacity of the three DERs is 80 KVA, 70 KVA and 60 KVA, respectively, and the three loads in the microgrid are modeled as constant power loads. We start the testing with the load's active and reactive power demand set to zero. Afterwards, the total active power demand in the microgrid is increased by 10 kW, in one-minute intervals, as depicted in Fig. 2. This is achieved by increasing $d_4(t)$, $d_5(t)$, and $d_6(t)$, successively, for about sixteen minutes.

B. C-HIL Testing Results

When there is no secondary frequency controller used, post any demand perturbation, we see that the frequency keeps lowering over time (see Fig. 3a). The DER injections into the microgrid increase according to the droop control laws (see Fig. 3b). When the proposed secondary frequency control scheme is deployed, we see that the frequency error is fixed post any demand perturbation, (see Fig. 4a). The associated increase in DER injections is shown in Fig. 4b.

V. Concluding Remarks

In this paper, we described a distributed secondary frequency control scheme for islanded AC microgrids with lossy networks. The scheme does not assume uniform resistance to reactance ratio for the electric distribution lines in the network. Although the results presented are for a microgrid with inverter-interfaced DERs, the scheme can work with any resource mix. In comparison to the work presented in [14], the proposed scheme utilizes far fewer control nodes as it only needs the monitoring of the DER buses in the microgrid. Thus, the proposed scheme is easily scalable for larger microgrid networks.

References

[1] A. D. Domínguez-García, C. N. Hadjicostis, and N. Vaidya, "Resilient networked control of distributed energy resources," *IEEE Journal on Selected Areas in Comm.*, vol. 30, no. 6, pp. 1137–1148, July 2012.

[2] D. Bakken, A. Bose, K. M. Chandy, P. P. Khargonekar, A. Kuh, S. Low, A. von Meier, K. Poolla, P. P. Varaiya, and F. Wu, "Grip - grids with intelligent periphery: Control architectures for grid2050$^{\pi}$," in *Proc. of the IEEE International Conference on Smart Grid Communications*, Oct. 2011, pp. 7–12.

[3] E. Mayhorn, L. Xie, and K. Butler-Purry, "Multi-time scale coordination of distributed energy resources in isolated power systems," *IEEE Transactions on Smart Grid*, vol. 8, no. 2, pp. 998–1005, Mar. 2017.

[4] R. H. Lasseter, "Microgrids," in *Proc. of the Power Engineering Society Winter Meeting*, vol. 1, 2002, pp. 305–308 vol.1.

[5] F. Katiraei and M. R. Iravani, "Power management strategies for a microgrid with multiple distributed generation units," *IEEE Transactions on Power Systems*, vol. 21, no. 4, pp. 1821–1831, Nov 2006.

[6] J. A. P. Lopes, C. L. Moreira, and A. G. Madureira, "Defining control strategies for microgrids islanded operation," *IEEE Transactions on Power Systems*, vol. 21, no. 2, pp. 916–924, May 2006.

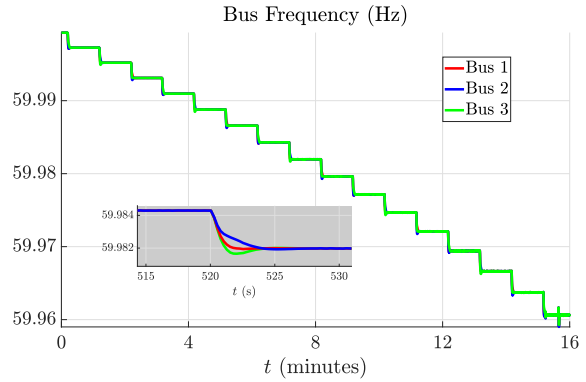

(a) Bus frequency response (no secondary frequency control).

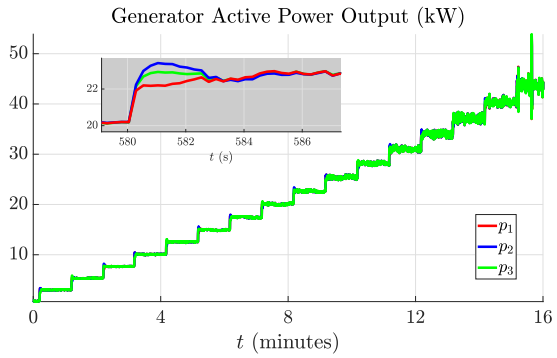

(b) Active power response (no secondary frequency control).

Fig. 3: System response (no secondary frequency control).

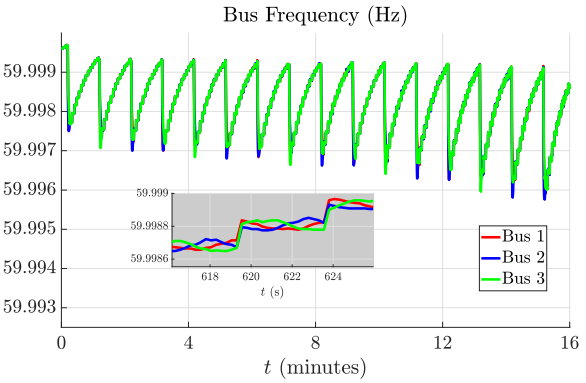

(a) Bus frequency response (with distributed secondary frequency control).

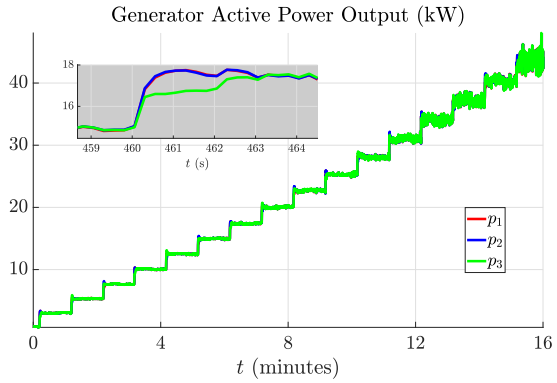

(b) Active power response (with distributed secondary frequency control).

Fig. 4: System response (with distributed secondary frequency control).

[7] J. M. Guerrero, J. C. Vasquez, J. Matas, L. G. de Vicuna, and M. Castilla, "Hierarchical control of droop-controlled ac and dc microgrids—a general approach toward standardization," *IEEE Transactions on Industrial Electronics*, vol. 58, no. 1, pp. 158–172, Jan 2011.

[8] J. M. Guerrero, J. C. Vasquez, J. Matas, M. Castilla, and L. Garcia de Vicuna, "Control strategy for flexible microgrid based on parallel line-interactive ups systems," *IEEE Transactions on Industrial Electronics*, vol. 56, no. 3, pp. 726–736, March 2009.

[9] A. D. Domínguez-García and C. N. Hadjicostis, "Distributed algorithms for control of demand response and distributed energy resources," in *Proc. of the IEEE Conference on Decision and Control*, 2011, pp. 27–32.

[10] S. T. Cady, A. D. Domínguez-García, and C. N. Hadjicostis, "Robust implementation of distributed algorithms for control of distributed energy resources," in *Proc. of the North American Power Symposium*, 2011, pp. 1–5.

[11] J. W. Simpson-Porco, F. Dörfler, and F. Bullo, "Synchronization and power sharing for droop-controlled inverters in islanded microgrids," *Automatica*, vol. 49, no. 9, pp. 2603 – 2611, 2013.

[12] S. T. Cady, A. D. Domínguez-García, and C. N. Hadjicostis, "A distributed generation control architecture for islanded ac microgrids," *IEEE Transactions on Control Systems Technology*, vol. 23, no. 5, pp. 1717–1735, Sep. 2015.

[13] F. Dörfler, J. W. Simpson-Porco, and F. Bullo, "Breaking the hierarchy: Distributed control and economic optimality in microgrids," *IEEE Transactions on Control of Network Systems*, vol. 3, no. 3, pp. 241–253, Sep. 2016.

[14] S. T. Cady, M. Zholbaryssov, A. D. Domínguez-García, and C. N. Hadjicostis, "A distributed frequency regulation architecture for islanded inertialess ac microgrids," *IEEE Transactions on Control Systems Technology*, vol. 25, no. 6, pp. 1961–1977, Nov. 2017.

[15] R. Salcedo, E. Corbett, C. Smith, E. Limpaecher, R. Rekha, J. Nowocin, G. Lauss, E. Fonkwe, M. Almeida, P. Gartner, S. Manson, B. Nayak, I. Celanovic, C. Dufour, M. O. Faruque, K. Schoder, R. Brandl, P. Kotsampopoulos, T. Ham Ha, A. Davoudi, A. Dehkordi, and K. Strunz, "Banshee distribution network benchmark and prototyping platform for hardware-in-the-loop integration of microgrid and device controllers," *The Journal of Engineering*, vol. 2019, no. 8, pp. 5365–5373, 2019.

[16] O. Ajala, A. D. Domínguez-García, and P. W. Sauer, *A Hierarchy of Models for Inverter-Based Microgrids*. New York, NY: Springer New York, 2018, pp. 307–332.

[17] M. Chandorkar, D. Divan, and R. Adapa, "Control of parallel connected inverters in standalone ac supply systems," *Industry Applications, IEEE Transactions on*, vol. 29, no. 1, pp. 136–143, 1993.

[18] K. De Brabandere, B. Bolsens, J. Van den Keybus, A. Woyte, J. Driesen, and R. Belmans, "A voltage and frequency droop control method for parallel inverters," *Power Electronics, IEEE Transactions on*, vol. 22, no. 4, pp. 1107–1115, 2007.

[19] S. T. Cady, A. D. Domínguez-García, and C. N. Hadjicostis, "Finite-time approximate consensus and its application to distributed frequency regulation in islanded ac microgrids," in *Proc. of the Hawaii International Conference on System Sciences*, Jan. 2015, pp. 2664–2670.

[20] C. N. Hadjicostis, N. Vaidya, and A. D. Domínguez-García, "Robust distributed average consensus via exchange of running sums," *IEEE Transactions on Automatic Control*, vol. 61, no. 6, pp. 1492–1507, June 2016.

[21] O. Azofeifa, S. Nigam, O. Ajala, C. Sain, S. Utomi, A. D. Domínguez-García, and P. W. Sauer, "Controller hardware-in-the-loop testbed for distributed coordination and control architectures," in *Proc. of North American Power Symposium, Wichita, KS*, Oct. 2019.